



HAL
open science

On the simulation of large viscoplastic structures under anisothermal cyclic loadings

Laetitia Verger, Andrei Constantinescu, Eric Charkaluk

► To cite this version:

Laetitia Verger, Andrei Constantinescu, Eric Charkaluk. On the simulation of large viscoplastic structures under anisothermal cyclic loadings. IUTAM Symposium on Creep in Structures, Apr 2000, Nagoya, Japan. pp.341-350, 10.1007/978-94-015-9628-2_33 . hal-00116226

HAL Id: hal-00116226

<https://hal.science/hal-00116226>

Submitted on 26 Sep 2022

HAL is a multi-disciplinary open access archive for the deposit and dissemination of scientific research documents, whether they are published or not. The documents may come from teaching and research institutions in France or abroad, or from public or private research centers.

L'archive ouverte pluridisciplinaire **HAL**, est destinée au dépôt et à la diffusion de documents scientifiques de niveau recherche, publiés ou non, émanant des établissements d'enseignement et de recherche français ou étrangers, des laboratoires publics ou privés.



Distributed under a Creative Commons Attribution - NonCommercial 4.0 International License

On the simulation of large viscoplastic structures under anisotropic cyclic loadings

L. VERGER^{1,2} (verger1@mpsa.com),
A. CONSTANTINESCU¹ (constant@lms.polytechnique.fr),
E. CHARKALUK³ (charkalu@mpsa.com)

¹ *Laboratoire de Mécanique des Solides (CNRS UMR 7649),
Ecole Polytechnique, 91128 Palaiseau, France*

² *P.S.A. Peugeot-Citroën – Direction des Techniques et Achats,
18 rue des Fauvelles, 92250 La Garenne-Colombes, France*

³ *P.S.A. Peugeot-Citroën – Direction de la Recherche et de
l'Innovation Automobile, Chemin de la Malmaison, 91570 Bièvres,
France*

Abstract. The optimal design of parts submitted to thermomechanical loadings is a key issue for the safety and quality assessments of structures. In this context, the present paper discusses the choice of a behavior model and the determination of its parameters. For cast iron and aluminum alloy applications, two constitutive laws are compared : one is based on a classical unified viscoplastic model and the other is based on a two-layer plastic-viscous rheological model. The following discussion shows that the use of anisothermal experiments is very important for the identification of material parameters and that simple models can be successfully applied for the predictive lifetime assessments of large 3D structures.

1. Introduction

Non-linear constitutive material behaviors have been the subject of extensive researches from the theoretical and numerical point of view over the last decades.

A large number of phenomenological models are devoted to the behavior of metals at high temperatures. They usually attempt to describe the metal-lurgical phenomena precisely [3,5]. However, they are not always suited for industrial design processes. Indeed, when computing cyclic multiaxial ther-

momechanical loadings on large structures, design engineers have to fulfill demands of predictive lifetime assessments within short design periods.

Then a complete computational design approach consists of three principal steps [1]:

- *The thermomechanical loading.* The mechanical analysis is based on numerical computations depending on the precise knowledge of the temperature history and boundary conditions. The temperature history is obtained from a combustion modeling and its following thermal transfer analysis.
- *The constitutive model.* The model should describe the behavior over the whole range of operating temperatures of the structure in isothermal as well as in anisothermal loading conditions. It has to be implemented in standard FEM computer codes using efficient and robust integration algorithms.
- *The lifetime prediction criterion.* The criterion is a low-cycle fatigue criterion in a multiaxial and anisothermal context. The criterion should also take into account the standard deviation due to the industrial manufacturing process.

The present paper focuses on the choice of a constitutive model in an anisothermal context and its underlying questions. Two important *a priori* assumptions are made concerning the model. We suppose on one hand that the cyclic softening/hardening behavior can be neglected and on the other hand that damage does not affect the material behavior during the main part of its life. In spite of the errors potentially induced by such assumptions, this leads to both shorter computation times and predictive final results [2,10].

Two metallic alloys will be discussed in the sequel: a spheroidal graphite *cast iron* (SiMo SG) with Mo and Si additions, used for exhaust manifolds in a 0 – 800°C temperature range, and an *aluminum-silicon alloy* (ASME A356) with Mg addition, used for cylinder heads in a 0 – 300°C temperature range.

For these alloys, both a unified model and a two-layer elastoviscoplastic model are presented, together with a summary of their numerical integration scheme.

A series of questions are discussed regarding the identification of the parameters of the models in an anisothermal context, the difficulty of choosing between the two models, the passage from 1D tension-compression tests to 3D structures and from isothermal loading conditions to anisothermal ones.

As a final conclusion, it is shown that complete FEM computations can be performed on structures in spite of some behavior-modeling uncertainties, and that subsequent results can be used for successful lifetime

predictions.

2. Constitutive models

The choice of the constitutive model is a key point in the global computational approach. It should represent the material behavior in the temperature and strain-rate range of the structure and it should be identified from a series of simple experiments on specimens.

2.1. EXPERIMENTS

The following experiments were at our disposal: *isothermal uniaxial tests* at different temperature levels which highlight the mechanisms of the phenomenological model ; *anisothermal uniaxial tests* which describe the transient behavior from room temperature to maximum temperature ; *anisothermal tests with temperature gradient* which exhibit a local state comparable with that of the complete structure.

The *uniaxial isothermal tests* are both tension-relaxation-compression tests (TRC) at different strain rates and low-cycle fatigue tests (LCF) characterizing the cyclic behavior and lifetime at different strain levels. The relaxation parts of the TRC stress/time data show exponential shapes (Fig. 1a). Therefore a Norton-Hoff power-law can be used for viscosity modeling. LCF data exhibit small cyclic softening which allows us to neglect isotropic hardening. Finally, cyclic TRC data and LCF data show a quick stabilization of the stress response (Fig. 1b). As a consequence, we shall assume that the damage undergone by the specimen at each cycle does not significantly affect the cyclic behavior.

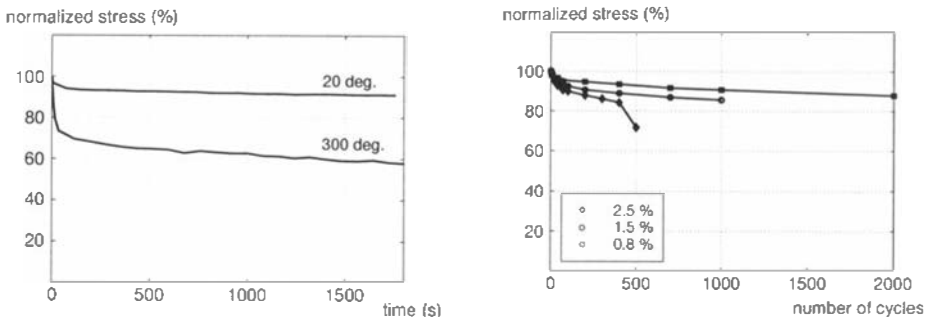


Figure 1. Experimental observations on *aluminum alloy* : (a) exponential shape of relaxation in TRC tests, (b) negligible cyclic softening behavior in LCF tests

The *anisothermal uniaxial tests* are difficult to perform but they provide important data for identification [7]. The difficulties stem from the simul-

taneous need of a homogeneous temperature field in the specimen and a precise and rapid control of temperature and strain rates.

In the case of the *aluminum alloy*, two testing conditions were defined:

- an out-of-phase compression with temperature ranging from 50°C to 300°C , which is used to fit the variation of characteristics with temperature,
- an out-of-phase compression with a pseudo-dwell at maximum strain and maximum temperature which enhances the influence of the viscosity at high temperature.

Finally, some *anisothermal tests with a temperature gradient along the specimen* were performed on a special machine [2]. The specimen was clamped between two cantilever beams and heated by Joule effect. The maximum temperature distribution along the *aluminum alloy* (respectively *cast iron*) specimen varies from 40°C at its ends to 300°C (respectively 700°C) in its middle section.

2.2. PHENOMENOLOGICAL VISCOPLASTIC MODELS

Two viscoplastic models have been deduced from the previous experimental observations using classical phenomenological formulations. They both take into account plastic behavior with a linear kinematic hardening rule and viscous behavior with a Norton-Hoff power law.

The first model is a *unified viscoplastic model (UM)* [4,5]. Viscosity and plasticity are represented by a single internal variable : the inelastic strain. The corresponding rheological representation is presented on Fig. 2.

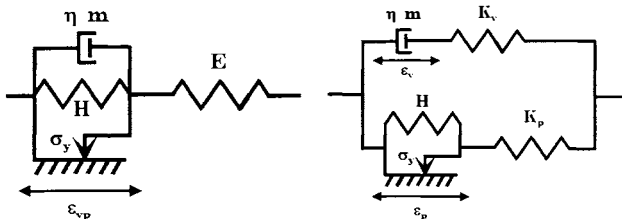


Figure 2. Rheological representation of the unified model (UM), and the two-layer model (TLM)

The second model is a *two-layer plastic-viscous rheological model (TLM)*, initially proposed by Kichenin [6]. The inelastic strain is represented by two independent internal variables.

The models are conditioned by temperature-dependent parameters which can be described as follows for 1D formulation: E , K_p and K_v are the elastic moduli of each layer, σ_y is the yield stress and H the hardening modulus, η is the viscosity coefficient and m the power coefficient of Norton-Hoff law.

2.3. CONSTITUTIVE LAWS

In the sequel, vectorial and tensorial variables are denoted by bold fonts. $\boldsymbol{\varepsilon}$ and $\boldsymbol{\sigma}$ stand for strain and stress tensors. In the *TLM* case, the subscripts *ev* and *ep* denote quantities related to viscous and plastic layers respectively.

The strain is supposed to decompose additively into elastic and inelastic parts:

$$\begin{array}{ll} (UM) & (TLM) \\ \boldsymbol{\varepsilon} = \boldsymbol{\varepsilon}^e + \boldsymbol{\varepsilon}^{vp} & \boldsymbol{\varepsilon} = \boldsymbol{\varepsilon}_{ev}^e + \boldsymbol{\varepsilon}_{ev}^v \\ & = \boldsymbol{\varepsilon}_{ep}^e + \boldsymbol{\varepsilon}_{ep}^p \end{array} \quad (1)$$

The stresses and hardening variables are linked to the strain variables by the following equations:

$$\begin{array}{ll} (UM) & (TLM) \\ \boldsymbol{\sigma} = \mathbf{C} : \boldsymbol{\varepsilon}^e & \boldsymbol{\sigma} = \boldsymbol{\sigma}_{ev} + \boldsymbol{\sigma}_{ep} \\ \mathbf{X} = -\mathbf{H} : \boldsymbol{\alpha} & \boldsymbol{\sigma}_{ev} = \mathbf{C}_{ev} : \boldsymbol{\varepsilon}_{ev}^e \\ & \boldsymbol{\sigma}_{ep} = \mathbf{C}_{ep} : \boldsymbol{\varepsilon}_{ep}^e \\ & \mathbf{X}_{ep} = -\mathbf{H}_{ep} : \boldsymbol{\alpha}_{ep} \end{array} \quad (2)$$

\mathbf{C} and \mathbf{H} denote the elasticity and hardening tensors. In this case, the hardening variable $\boldsymbol{\alpha}$ is equal to the cumulated plastic strain.

The von Mises equivalent stress is used to define the plasticity criterion:

$$J_2(\mathbf{s}) = \sqrt{\frac{3}{2} (\mathbf{s} : \mathbf{s})} \text{ where } \mathbf{s} = \text{dev} \boldsymbol{\sigma}.$$

Then the flow-rules can be expressed under the following form:

$$\dot{\boldsymbol{\varepsilon}}^{in} = \gamma \cdot \frac{\mathbf{A}}{\sqrt{\mathbf{A} : \mathbf{A}}} \quad (3)$$

where:

$$\begin{array}{ll} (UM) & (TLM) \\ \mathbf{A} = \text{dev}(\boldsymbol{\sigma} - \mathbf{X}) & \mathbf{A}_{ev} = \text{dev}(\boldsymbol{\sigma}_{ev}) \\ \mathbf{X} = -\frac{2}{3} \mathbf{H} : \boldsymbol{\varepsilon}^{vp} & \mathbf{A}_{ev} = \sqrt{\frac{3}{2}} \left\langle \frac{J_2(\mathbf{A}_{ev})}{\eta} \right\rangle^m \\ \gamma = \sqrt{\frac{3}{2}} \left\langle \frac{J_2(\mathbf{A}) - \sigma_y}{\eta} \right\rangle^m & \mathbf{A}_{ep} = \text{dev}(\boldsymbol{\sigma}_{ep} - \mathbf{X}_{ep}) \\ & \mathbf{X}_{ep} = -\frac{2}{3} \mathbf{H}_{ep} : \boldsymbol{\varepsilon}_{ep}^p \end{array} \quad (4)$$

For theoretical details of the presented thermodynamical framework, see [5].

The constitutive equations have been integrated by an implicit Newton-Raphson integration scheme using a return-mapping algorithm and consistent tangent moduli [8,9].

3. Identification of material parameters

3.1. A CLASSICAL APPROACH

In a first stage, the parameters have been directly estimated from the stabilized isothermal TRC data. The identification was based on some simple interpretations of the physical meaning of the parameters: the elastic and hardening moduli are slopes read on stress/strain tension curves, the viscosity parameters fit the relaxation curve, the yield stress is found from the relaxed stress, etc. The temperature-dependent parameters were obtained by a linear interpolation between the TRC temperatures.

In the *cast iron* case, the parameters have been determined as described above, and afterwards they have been used to simulate the anisothermal clamped test. The local stress/strain state in the specimen is multiaxial due to the temperature gradient along its axis. The computed and measured axial stresses are in a reasonable accordance (Fig. 3a), but there is a difference in the radial stress/strain responses between the (*UM*) and the (*TLM*) models (Fig. 3b). All the same, the numerical results obtained for

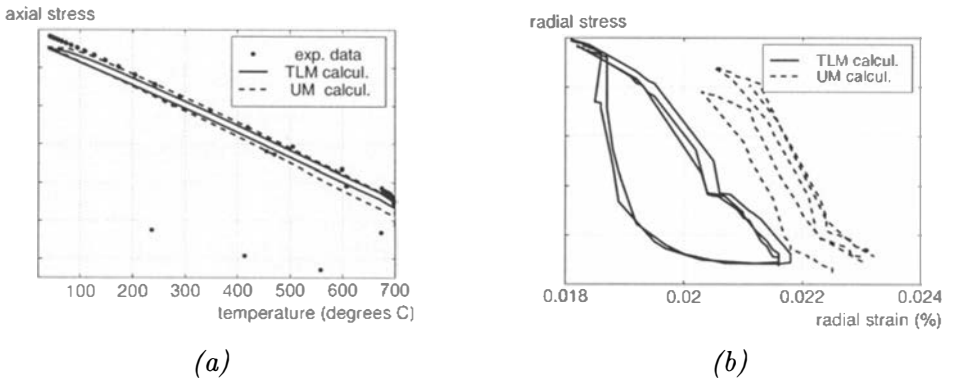


Figure 3. Anisothermal clamped test for *cast-iron*: (a) experimental/computed data comparison on a stabilized cycle (b) computational data comparison for two models

cast iron with the (*TLM*) model permitted correct lifetime predictions on exhaust manifolds [2,10].

The understanding of the differences between the behavior of the two models during the simulation of the clamped test is not an easy task. A first difficulty comes from the experiment, in which the stress and strain fields are controlled by a complex temperature distribution. The transient temperature field has to be computed very precisely in order to obtain accurate results for the mechanical fields. Moreover, due to the 3D nature of the fields, it is particularly difficult to read the sensitivities of the models and parameters with regard to the loading.

The second difficulty comes both from the models and the isothermal identification method. Indeed both models inherit an indetermination between the plastic and the viscous quantities (Fig. 4), which implies that the evolution of the parameters with temperature is badly managed. Therefore the prediction of the anisothermal mechanical response may be dubious.

In conclusion, we should find a simpler way to enhance identification. A better experiment should exhibit a homogeneous temperature field. Then the computed identification problem would be a 1D problem, much easier to analyze. This is the case of the anisothermal experiments without gradient described above. We should also dispose of a more general identification procedure permitting the combination of isothermal and anisothermal tests data.

3.2. AN OPTIMAL CONTROL APPROACH

In the sequel the identification of the material parameters is essentially based on the minimization of a cost functional defined as:

$$J(p) = \frac{1}{2} \int [\sigma_{exp}(t) - \sigma_{calc}(p, t)]^2 dt$$

where the time-integral measures the difference between the experimental and computed stresses (σ_{exp} and σ_{calc} respectively) over a complete experiment. In order to determine parameters from several experiments, the corresponding cost functionals can be added using weight factors.

The minimization procedure was based on a gradient computation using the adjoint state method and a BFGS gradient descent algorithm. This procedure can be combined with direct calibration of elastic and hardening moduli from the slopes of the isothermal curves as described in section 3.1.

The indetermination related to competition between plastic and viscous quantities is illustrated by plotting the cost functional as a function of the viscous parameters (η, m) (Fig.4). In the case of an isothermal tensile test, one can remark a long flat valley proving the coupling effect between the two parameters as well as the laborious identification induced.

Several identifications showed that a complete parameters set can be determined from a single anisothermal experiment (Fig. 5b). However, a single experiment will generally not assure the validity of the set in all test conditions. Therefore one should combine isothermal and anisothermal experiments in the identification program. This combination conducts to a difficult multiobjective minimization, where the identified parameters set will depend on the weight attributed to the different experiments.

In spite of these difficulties, the final parameters obtained by this method permitted several reasonably accurate computations on structures as presented in the next section.

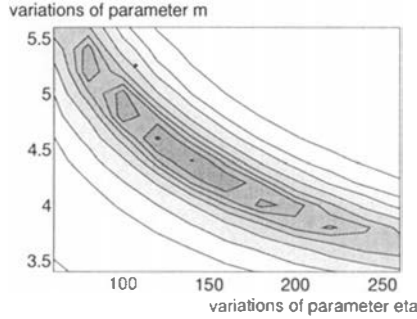


Figure 4. Cost functional distribution for three isothermal tests with aluminum alloy

4. Computations on structures

The computations on structures have been realized using the ABAQUS Standard FEM code after the determination of the parameters using the previous techniques.

The global computational approach is based on an important assumption: as for plastic shakedown phenomena, we assume that the response of the structure will rapidly stabilize under cyclic thermomechanical loadings. The stabilized computed cycle is generally obtained after a few cycles (< 10) and the corresponding mechanical fields are used as the input of the fatigue analysis.

The FEM meshes for exhaust manifolds or cylinder heads had $\approx 10^4 - 10^5$ degrees of freedom. The thermomechanical computations were completed within approximately 6 hours of CPU time on a HP-V class computer. The CPU time showed to be very sensitive both to nonlinearities of the constitutive model and to the contact boundary conditions.

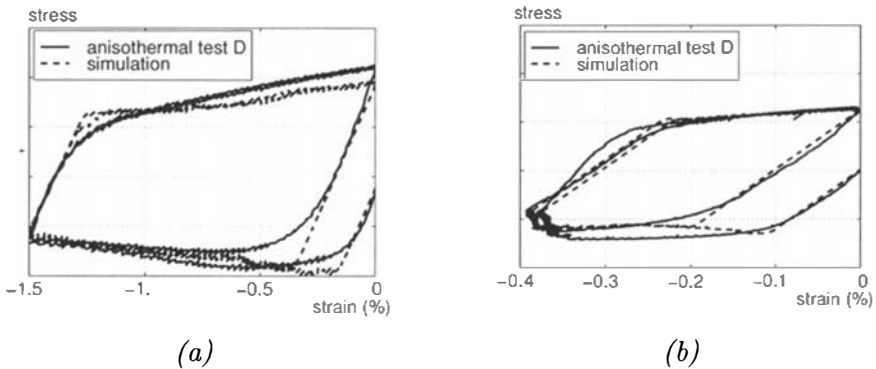


Figure 5. Experimental and computed anisothermal uniaxial test with parameters identified from: (a) isothermal and anisothermal tests, (b) anisothermal tests

In the case of *cast-iron* exhaust manifolds, parameters of the constitutive models are identified using the classical method. Once more, there is a difference between the stress/strain responses of the *UM* and *TLM* models. Using an energy-based criterion for thermomechanical fatigue [2], the results from the *TLM* model permitted to determine the lifetime of several 3D structures: the clamped specimen under four test conditions and three exhaust manifold geometries (Fig.7). This shows the reliability of the presented global approach in thermomechanical fatigue.

In the case of *aluminum alloy* cylinder heads, parameters of the constitutive models are determined using the optimal control approach including anisothermal tests. 3D computations have been conducted on a one-cylinder head prototype for one particular test configuration.

A numerical comparison in the case of the clamped specimen shows a small difference in the mechanical response between the two models (Fig. 6). This proves the great importance of using anisothermal tests for the identification of the parameters. The lifetime results are not available yet to validate the global approach in the case of the *aluminum alloy* cylinder heads.

5. Conclusion

This paper discussed some problems related to the choice and the identification of a constitutive law for thermomechanical computations on real 3D structures. A series of difficulties have exhibited the importance of using anisothermal tests during the identification process. The encouraging results show that simple constitutive laws are sufficient for a robust lifetime prediction in an industrial context.

Acknowledgement to A. Bignonnet (PSA) and K. Dang Van (LMS) for encouraging this project and G. Lederer (PSA) for continuous support.

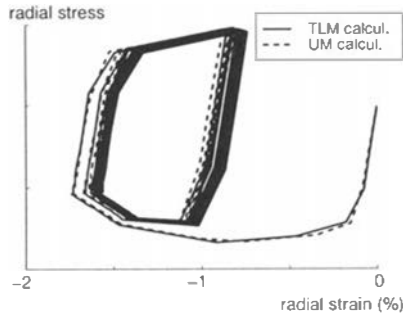


Figure 6. Comparison of the stress/strain curves for the two models in the case of aluminum clamped specimen

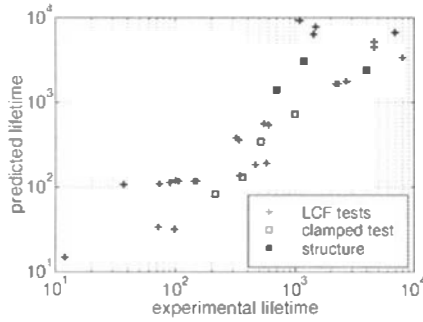


Figure 7. Lifetime assessments for cast-iron structures (exhaust-manifolds)

References

1. E. CHARKALUK, A. CONSTANTINESCU, A. BIGNONNET AND K. DANG VAN in *Low cycle fatigue and elasto-plastic behavior of materials*, ed. K.T. Rie et P.D. Portella, Elsevier, 1998, pp 815–820.
2. E. CHARKALUK, A. CONSTANTINESCU, An energetic approach in thermomechanical fatigue for silicon molybden cast iron, accepted for publication in *J. Mat. High. Temp.*, 2000
3. D. FRANCOIS, A. PINEAU, A. ZAOUJ in *Comportement mécanique des matériaux - vol II*, Hermès, Paris, 1994
4. J.L. CHABOCHE, Sur l'utilisation des variables d'état interne pour la description du comportement viscoplastique et de la rupture par endommagement, *Symposium Franco-Polonais de Rhéologie et de Mécanique*, 1977
5. J. LEMAITRE AND J. L. CHABOCHE, *Mécanique des matériaux solides*, Dunod, Paris, 1985
6. J. KICHENIN, *Comportement thermomécanique du polyéthylène - Application aux structures gazières*, PhD Thesis, Ecole Polytechnique (France), 1992
7. L. REMY Thermal and thermal-mechanical fatigue of superalloys - a challenging goal for mechanical tests and models, in *Low cycle fatigue and elasto-plastic behaviour of materials*, ed. K.T. Rie et P.D. Portella, Elsevier, 1998, pp 119–130
8. J.C SIMO and T.J.R. HUGHES, *Computational Inelasticity*, Springer Verlag, 1998
9. E. CHARKALUK, L. VERGER, A. CONSTANTINESCU, G. LEDERER AND C. STOLZ, Lois de comportement viscoplastiques anisothermes pour calculs cycliques sur structures, *Colloque Nat. en Calcul des Structures*, ed. Guédra-Degeorges and Co., 1999, pp. 575–580
10. G., LEDERER, E. CHARKALUK, L. VERGER, A. CONSTANTINESCU, Numerical life assessment of engine parts submitted to thermomechanical fatigue - Application to exhaust manifolds, *SAE Technical paper series*, 2000-01-0789